Miscibility and morphology of binary polymer blends of polycaprolactone with solution-chlorinated polyethylenes

G. Defieuw, G. Groeninckx* and H. Reynaers
Laboratory of Macromolecular Structural Chemistry, Katholieke Universiteit Leuven, Celestijnenlaan 200F, 3030 Heverlee, Belgium
(Received 17 June 1988; revised 7 September 1988; accepted 12 October 1988)

Binary blends of solution-chlorinated polyethylenes (CPE) with polycaprolactone (PCL) were prepared by the coprecipitation technique. The phase behaviour of the mixtures was determined using optical microscopy, light transmission measurements, dynamic mechanical analysis and differential scanning calorimetry. The superstructure of the semicrystalline CPE/PCL blends was studied by small-angle X-ray diffraction, while the melting behaviour of PCL in the blends was investigated by differential scanning calorimetry. The miscibility was found to be dependent on the chlorine content of CPE and the temperature, while CPE is segregated interfibrillarly or interspherulitically during the crystallization of PCL in the blend. The double melting behaviour is attributed to a secondary crystallization process.

(Keywords: miscibility; semicrystalline morphology; blends)

INTRODUCTION

During the last few years, there has been an increasing interest in the use of polymer blends for technological applications. As a logical consequence, many studies have been devoted to polymer blends, with special emphasis on their mechanical and thermal behaviour. Relatively few studies, however, deal with the fundamental aspects of polymer miscibility and the resulting morphology of polymer blends.

Binary blends that have been studied extensively by various experimental techniques are poly(vinyl chlorine)/polycaprolactone (PVC/PCL)[1–4], poly(vinylidene fluoride)/poly(methyl methacrylate) (PVF_2/PMMA)[5,6] and poly(phenylene oxide)/polystyrene (PPO/PS)[7]. The binary system PVC/PCL seems to be miscible over the entire composition range and exhibits no lower critical solution temperature (*LCST*). By decreasing the chlorine content, one should be able to pass into a partially miscible or immiscible system, chlorinated polyethylene/polycaprolactone (CPE/PCL).

Many studies have been done concerning the crystallization behaviour and crystalline morphology of the binary polymer blend PVC/PCL. Ong and Price[4] suggested that this blend is amorphous and apparently miscible at high PVC concentrations. At lower PVC concentrations, crystallization of PCL occurs; this leads to volume-filling spherulites containing PVC within the spherulites. Concomitantly, a melting-point depression of PCL was observed in the presence of PVC as well as a substantial decrease of the rate of crystallization. Stein *et al.*[2,3] studied the semicrystalline morphology of PVC/PCL blends mainly by small-angle X-ray scattering (SAXS) and small-angle light scattering (SALS). These authors concluded that the crystalline PCL lamellae in the blends are separated by amorphous regions containing mixed PVC and PCL. Maxima in the light scattering patterns, beyond the typical H_v and V_v pattern, were interpreted in terms of periodical twisting of the crystalline lamellae.

Since the slurry-phase suspension chlorination process of linear polyethylene yields a multiblock segmented structure which is extremely complex, solution chlorination was preferred to prepare randomly chlorinated polyethylenes with a uniform molecular structure.

In the present study, PVC has been substituted by amorphous solution-chlorinated polyethylenes (CPE) and their melt miscibility with PCL has been investigated as a function of both the chlorine content of CPE and the temperature using optical microscopy, dynamic mechanical analysis and differential scanning calorimetry. The crystallization and melting behaviour and the semicrystalline morphology of these blends were studied by optical and electron microscopy, small angle X-ray scattering and differential scanning calorimetry.

EXPERIMENTAL

Materials

Chlorinated polyethylenes with different chlorine contents were obtained by bubbling chlorine gas through a 1% (w/v) solution of high-density polyethylene (HDPE) with two different molecular weights in 1,1',2,2'-tetrachloroethane at 110°C. A literature study[8] reveals that CPE obtained via solution chlorination exhibits a random distribution of the chlorine atoms along the backbone. The chlorine content of CPE was determined by elemental analysis (Schöninger method) and is given in weight per cent (mentioned after the name CPE).

From d.s.c. measurements it could be derived that CPE with a chlorine content of 30.1 wt% is already completely amorphous. In this work, only amorphous CPE has been used in blends with PCL.

The average molecular weights of CPE and PCL were determined by g.p.c. analysis relative to polystyrene

* To whom correspondence should be addressed

0032-3861/89/040595-09$03.00

Table 1 Molecular weight characteristics of the blend components as obtained by g.p.c. analysis relative to polystyrene standards

Sample	$\overline{M_w}$	$\overline{M_n}$	$\overline{M_w}/\overline{M_n}$	T_g (°C)
CPE35.6	198000	59000	3.35	−10
CPE42.1	193000	50000	3.84	1.5
CPE49.1	293000	53000	4.64	18.5
PCL	22500	14000	1.60	−63

standards using tetrahydrofuran (THF) as solvent. These results are summarized in *Table 1*. Blends were prepared by coprecipitation of a 3% (w/v) THF solution in hexane. This method of preparation was preferred instead of melt mixing because it allows one to obtain blends that are mixed on a molecular level. Moreover, the choice of the solvent and the non-solvent does not affect the state of miscibility as is the case in solvent-cast films.

Techniques

D.s.c. scans for the investigation of the glass transition temperature and the melting behaviour of the blends were run at a heating rate of 5°C min^{-1} on a Perkin-Elmer DSC 2C equipped with a Thermal Analysis Data System (TADS). Prior to dynamic mechanical analysis (d.m.a.), the powdered blends were compression moulded at 120°C. The d.m.a. experiments were performed on a Dupont 1090 instrument at a scanning rate of 5°C min^{-1}.

The spherulitic growth rate of PCL in the PCL-rich blends was determined using optical microscopy. Powdered blends were molten in a Mettler FP2 or FP82 hot stage at 180°C for 5 min unless otherwise indicated, immediately followed by isothermal crystallization in the temperature range 35–45°C.

Samples for SAXS were prepared by compression moulding of powdered blends at 140°C. SAXS patterns were recorded photographically using an Anton Paar type Kratky camera provided with a 60 μm entrance slit resulting in a theoretical resolution of 1200 Å. The Philips PW1130 X-ray generator was operated at 45 kV and 30 mA; a Kratky-type Cu target in conjunction with a Ni β-filter was used throughout. Typical irradiation times were of the order of 3 to 15 h depending on sample thickness and absorption coefficient. All small-angle scattering information was obtained at room temperature as slit-smeared data in the infinite slit approach.

A Joyce-Loebl microdensitometer was especially adapted for reading the small-angle patterns on the film (Agfa-Gevaert Structurix D7) by uncoupling the driving servomotor of the registration and specimen tables and by intercalating a computer-steered step motor. The tracing pen holder was coupled with a nylon fibre to a potentiometer, the voltage recording of which was fed to an Apple IIE PC after digitization. Because the potentiometer readings are on an arbitrary scale, these values were brought onto an absolute scale in optical density (o.d.) by a set of Scott-Jena grey glasses of known optical density. All measurements referred to the o.d. of the film background measured at several parts of the film and those o.d. values were transformed into exposure values using equation (8) of ref. 9. The microdensitometer was always operated with the maximum slit height available (0.8 mm). Further data processing was done by the program FFSAXS5[9]. This includes subtraction of a linear background fitted to the tail of the scattering curve and a desmearing operation followed by multiplication with s^2 ($s=2\sin\theta/\lambda$), the so-called Lorentz factor. Direct analysis was supplemented by the calculation of the experimental one-dimensional correlation function obtained by Fourier transformation of the scattering curve, normalized in such a way that $\gamma_1(r=0)=1$.

Procedures to evaluate correlation functions have been proposed and discussed by Vonk and Strobl[9,10].

Transmission electron microscopic investigations were made on ultramicrotomed sections which were obtained at −140°C from the SAXS samples using an LKB ultramicrotome equipped wth a cryogenic unit. Owing to the presence of chlorine, there is no need for a staining technique.

RESULTS AND DISCUSSION

Miscibility of CPE with PCL

Miscible systems. Cloud-point observations by optical microscopy can give a first indication of the degree of miscibility of the blends studied. CPE49.1 is miscible with PCL over the entire composition and temperature range, while CPE42.1 exhibits a temperature- and composition-dependent miscibility (*Figure 1*). The cloud-point curve of CPE42.1/PCL is located at the PCL side owing to the difference in molecular weight between both polymers[11]. The reversibility of the phase separation process will be discussed further in this article.

Since miscible polymer blends exhibit a single glass transition temperature located between those of the pure components, d.s.c. measurements can give information about the state of miscibility. In order to obtain amorphous samples, blends were heated to 100°C and subsequently quenched in liquid nitrogen. Samples containing more than 80 wt% PCL were not completely amorphous after quenching. As can be seen from *Figure 2*, no broadening of the glass transition region is observed and the T_g data for these miscible systems fit rather well with the Fox equation (*Figure 3*). The thermal curves in *Figure 2* deflect after the T_g region in the CPE/PCL 30/70 and 50/50 blends, indicating that fast crystallization is taking place.

D.m.a. experiments on CPE49.1/PCL blends were performed using quenched amorphous and semicrystalline samples (*Figure 4*). The amorphous 50/50 blend exhibits only one glass transition peak intermediate between those of the pure components. The tan δ peak is shifted to higher temperatures after the crystallization of PCL due to the change in composition of the amorphous phase.

A study of the crystallization kinetics of the blends gives other indications for the presence of a miscible melt.

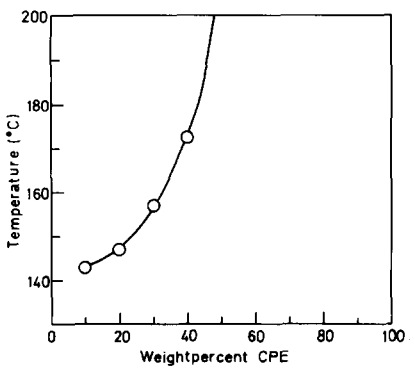

Figure 1 Cloud-point curve of CPE42.1/PCL blend

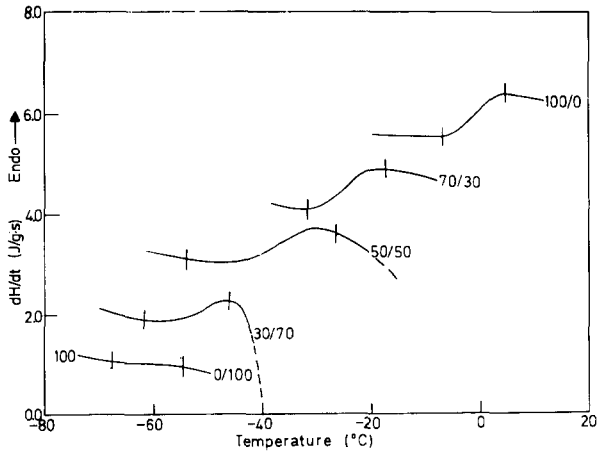

Figure 2 D.s.c glass transitions of amorphous CPE42.1/PCL blends

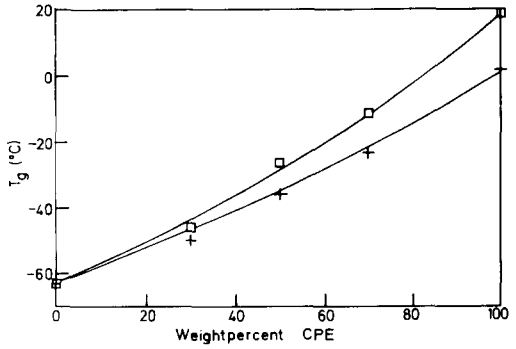

Figure 3 D.s.c. glass transition temperatures of amorphous CPE49.1/PCL (□) and CPE42.1/PCL (+) blends

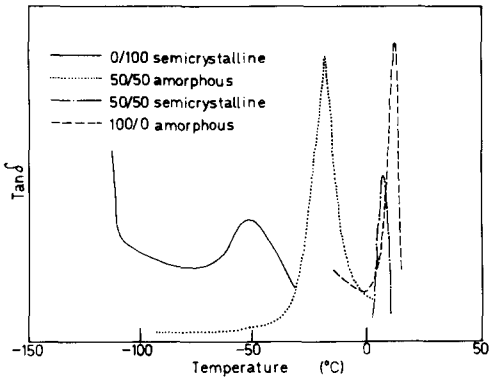

Figure 4 D.m.a. of CPE49.1/PCL blends

The spherulitic growth rate of PCL in the blends depends on both the CPE content (*Figure 5*) and the chlorine content (*Figure 6*). The spherulitic growth rate of PCL is affected much more by addition of CPE49.1 than by addition of CPE42.1, since CPE49.1 has a higher glass transition temperature. The depression of the growth rates can also be caused by a thermodynamic melting-point depression, but experimental data on the χ parameters are not available.

Although the phase separation process in CPE42.1/PCL should be reversible from the thermodynamic point of view, kinetic factors can strongly affect the reversibility. Indeed, phase-separated CPE42.1/PCL blends become optically clear below the *LCST*, but it takes more time to re-form the uniformly mixed melt. This is easily proved by measuring the spherulitic growth rate in the CPE42.1/PCL 20/80 blend kept above and below the *LCST* (147°C) before isothermal crystallization at 45°C (*Figure 7*). If the phase separation were completely reversible within this short time interval of spherulitic growth, the same spherulitic growth rate should be found for both samples. However, a higher spherulitic growth rate has been observed for the phase-separated blend than for the sample kept below the *LCST*. As the molten PCL-rich phase in the blend after the phase separation above *LCST* contains more PCL than the melt kept below *LCST*, a higher spherulitic growth rate is found in the former case.

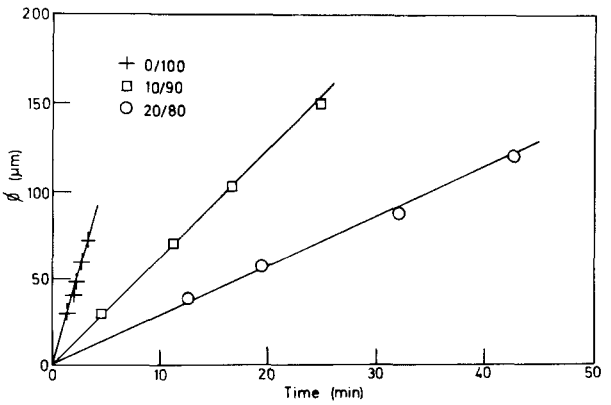

Figure 5 Spherulitic growth rate of CPE42.1/PCL blends at $T_c = 45°C$

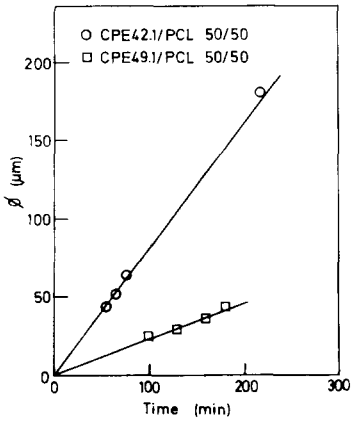

Figure 6 Spherulitic growth rate of CPE/PCL 50/50 blends at $T_c = 35°C$

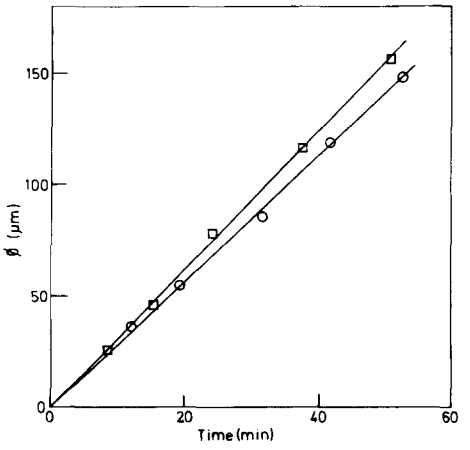

Figure 7 Spherulitic growth rate of CPE42.1/PCL 20/80 blend molten above and below the *LCST* (147°C): (□) $T = 180°C$, 5 min → $T_c = 45°C$; (○) $T = 140°C$, 5 min → $T_c = 45°C$

Partially miscible systems. For the chlorine contents of CPE below 42.1 wt%, the cloud-point curve is shifted to lower temperatures; a partially miscible blend at room temperature results when the minimum of this curve is located below room temperature. At 100°C, two phases are present in the CPE35.6/PCL 50/50 blend (*Figure 8a*) and the small domains resulting from the phase separation seem to fuse at higher temperatures (*Figure 8b*). The composition of both phases will also be different at the various temperatures studied, but the composition of both phases is difficult to determine. All compositions of the CPE35.6/PCL blend, which are separated into partially miscible coexisting phases, crystallize during the quenching process, since PCL crystallizes fast in the absence of amorphous diluent. Consequently, measurement of the glass transition temperatures of the partially miscible blends with d.s.c. is rather difficult.

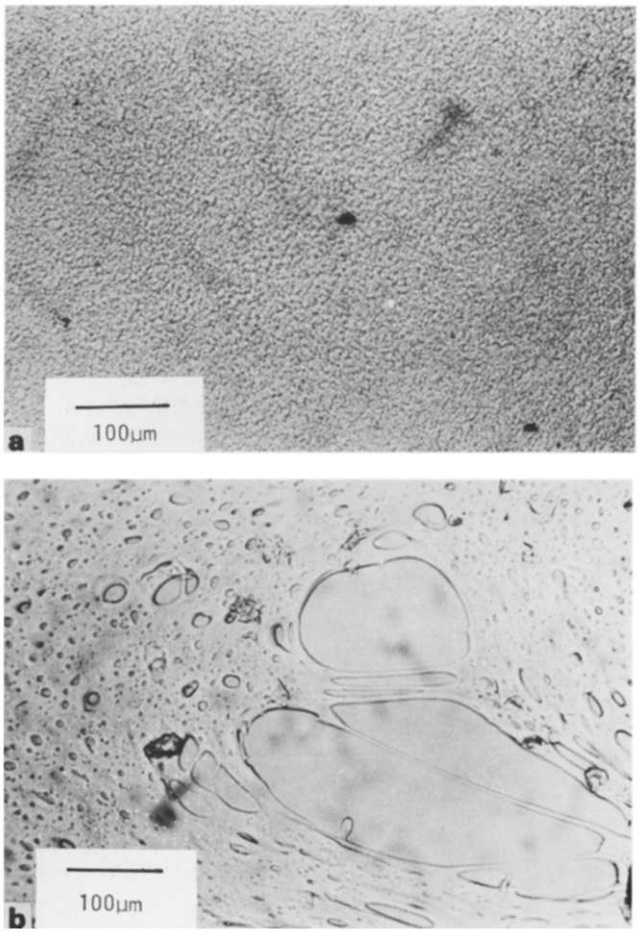

Figure 8 Melt morphology of CPE35.6/PCL 50/50 blend at different temperatures: (a) $T=100°C$; (b) $T=200°C$

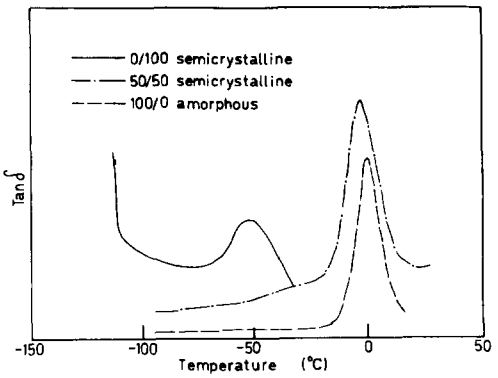

Figure 9 D.m.a. of CPE35.6/PCL blends

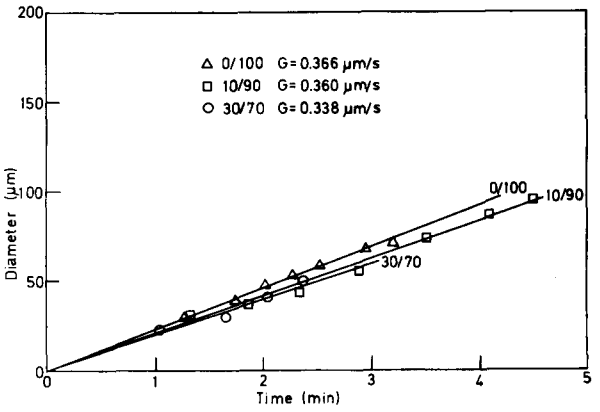

Figure 10 Spherulitic growth rate of CPE35.6/PCL blends at $T_c=42°C$

Only one tan δ peak corresponding to the glass transition of the CPE-rich phase is observed in d.m.a. experiments (*Figure 9*). The glass transition of the PCL-rich phase is not easily detectable due to the high degree of crystallinity of this phase. The presence of a small amount of CPE in the PCL-rich phase can be proved by measuring the spherulitic growth rate of PCL in this phase; a small decrease is observed for all compositions (*Figure 10*).

Since CPE35.6/PCL 90/10 forms a one-phase system at 100°C, as can be observed from optical microscopy and cloud-point measurements, while the 10/90 blend is phase-separated under the same conditions, one can conclude that the solubility of PCL in CPE is higher as compared to the latter blend. This can tentatively be accounted for by the pronounced differences in molecular weight of the polymers used[11].

Semicrystalline morphology of CPE/PCL blends

Optical microscopic observations. Evidence for intraspherulitic segregation of the amorphous component CPE is obtained by measuring the spherulitic growth rate of PCL in the CPE/PCL blends and by examination of the morphology at the end of the primary crystallization. It is well known from the literature data that PVC/PCL blends exhibit ring-shaped volume-filling spherulites at PVC concentrations below 50 wt%[1,12], and that the periodicity of twisting of the lamellae is a function of the blend composition.

In the miscible CPE/PCL blends, however, a ring-shaped spherulitic structure is only observed at very low CPE concentrations (*Figure 11*). The higher the CPE content, the more a disordered, dendritic structure is observed (*Figure 12*), which is very similar to the textures observed in aPS/iPS and iPP/aPP blends[13]. At these high PCL concentrations (between 70 and 100 wt% PCL), the spherulites are always volume-filling and consequently the amorphous CPE component must be segregated interlamellarly or interfibrillarly. At CPE contents above 30 wt%, one observes interspherulitic segregation of CPE (*Figure 13*) and this segregation phenomenon depends strongly on the crystallization temperature (*Figure 14*). This can be understood in terms of the semiquantitative δ-parameter approach introduced by Keith and Padden which is defined as:

$$\delta = D/G$$

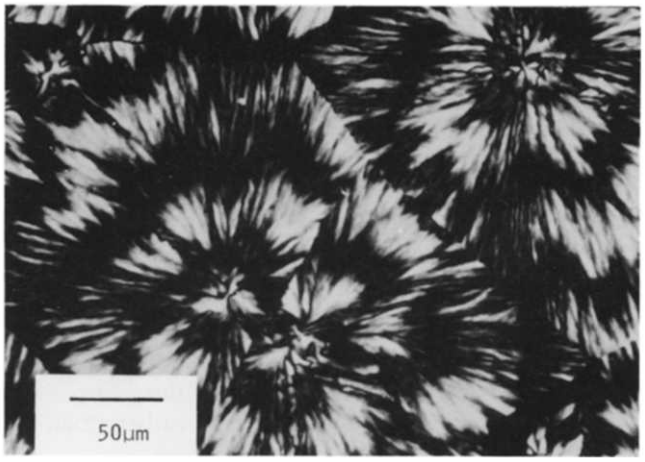

Figure 11 Spherulitic morphology of CPE49.1/PCL 10/90 after isothermal crystallization of PCL at 45°C

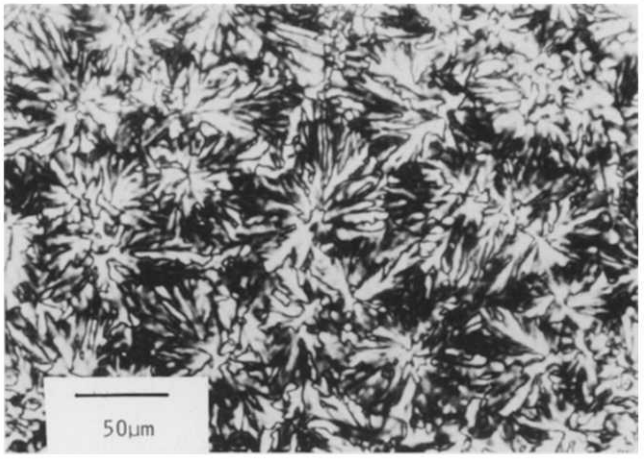

Figure 12 Spherulitic morphology of CPE49.1/PCL 20/80 after isothermal crystallization of PCL at 45°C

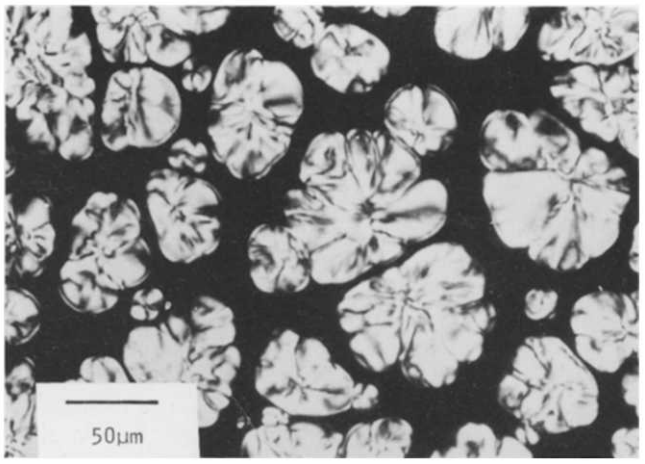

Figure 13 Spherulitic morphology of CPE49.1/PCL 50/50 after isothermal crystallization of PCL at 40°C

Here D represents the diffusion coefficient of the amorphous component and G is the spherulitic radial growth rate of the crystallizable component. The diffusion coefficient D increases at higher crystallization temperatures owing to the lower melt viscosity. In this study, all the crystallization temperatures used are close to the equilibrium melting temperature of PCL ($T_m^\circ = 63°C$), and secondary nucleation is therefore the rate-determining factor for the crystallization kinetics. An increase of the crystallization temperature thus results in a decrease of the growth rate of the crystalline PCL lamellae. Hence, both factors, diffusion and spherulitic growth kinetics, contribute to the increase of the δ parameter if the crystallization temperature is increased and result in a larger-scale segregation of the amorphous CPE component (interspherulitic instead of interfibrillar or interlamellar).

Small-angle X-ray scattering measurements. As can be inferred from investigations by optical microscopy, amorphous CPE is segregated interlamellarly or interfibrillarly at high PCL concentrations (70 to 100 wt%). Interlamellar segregation of the amorphous diluent between the crystalline lamellae will result in an increase of the structural long spacing L; this has been observed in a number of cases for polymer blends, such as PVC with PCL[1], iPS with PPO[7] and SAN with PCL[14].

Interfibrillar segregation on the other hand has no influence on the thickness of the amorphous phase between the crystalline lamellae and the long spacing L does not change. This type of segregation of the amorphous component has been reported for iPS/aPS blends[15].

The influence of the CPE concentration in the semicrystalline blends on the lamellar texture, as explored by SAXS, has been studied for different chlorine contents of CPE. In the partially miscible system CPE35.6/PCL, the PCL-rich phase gives the main contribution to the SAXS scattering pattern since the CPE-rich phase has only a very low degree of crystallinity (only $\sim 2\%$ as estimated from the d.s.c. thermogram of CPE35.6/PCL 90/10). No significant changes of the scattering pattern, the long spacing L and the one-dimensional correlation function could be observed by addition of CPE, since PCL crystallizes in the presence of very small amounts of CPE (*Figures 15* and *16*).

With respect to the correlation functions, all these and subsequent ones are in their general shape typical of non-ideal two-phase structures, exhibiting a number of characteristic features which can be interpreted on the basis of model calculations[10]. Some bending is observed at the origin of the correlation functions which is typical for a transition zone between the phases. A central linear section is observed in the self-correlation region pointing

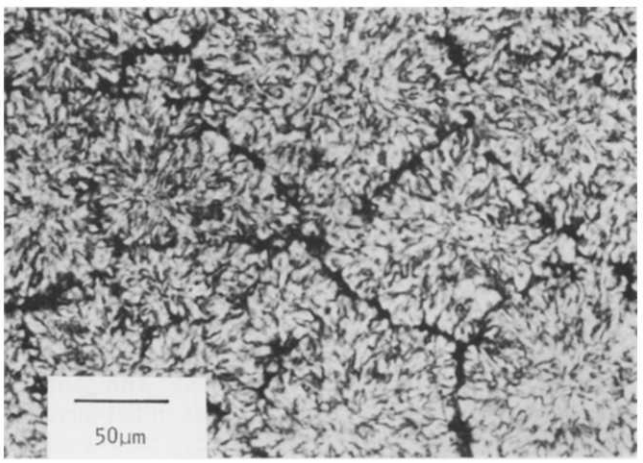

Figure 14 Spherulitic morphology of CPE49.1/PCL 50/50 after isothermal crystallization of PCL at 35°C

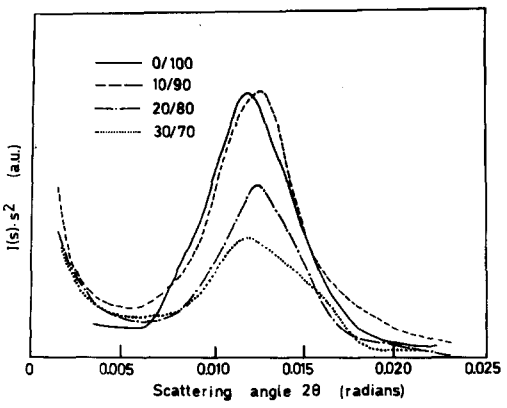

Figure 15 Lorentz-corrected desmeared SAXS curve of CPE35.6/PCL blends, isothermally crystallized at 40°C

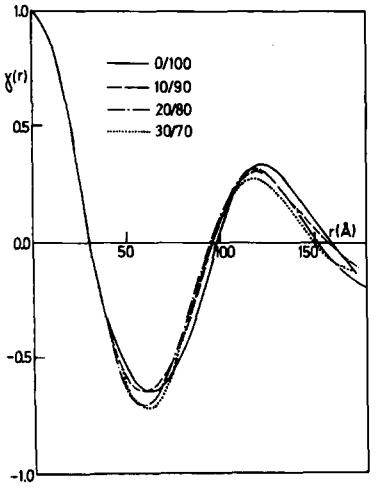

Figure 16 One-dimensional correlation function of CPE35.6/PCL blends after isothermal crystallization of PCL at 40°C for 14 days

to a substantial crystal core thickness. At higher values of r, one observes in all cases the maximum characterizing the correlation between next-neighbour lamellae, the peak value being representative for the mean long spacing of the superstructure. Unfortunately, no baseline shows up at the intermediate region between the first intersection of the correlation function with the r axis and the position of the long spacing. This situation is typical for samples with crystallinities between 20 and 70%. As a general rule, SAXS is not very sensitive for values of $x_c(1-x_c)$ in the vicinity of 0.25. Moreover, even in the case that the baseline coordinate can be estimated by means of other information (density data), small errors in the former parameter always result in large errors of x_c and the mean lamellar thickness. Consequently, a more elaborate analysis of the correlation function is hardly possible.

In the miscible CPE42.1/PCL blends, a small initial increase of the long spacing is observed up to 10 wt% CPE, but the long spacing decreases at higher CPE contents (*Figures 17* and *18*). This initial increase can be attributed to a small amount of CPE incorporated between the crystalline PCL lamellae, which causes the lamellae to twist during crystallization as already previously reported and in agreement with optical microscopic investigations. Although the initial increase is very small, the same shape of the long period *versus* composition curve has also been observed for phenoxy/PCL blends[16].

At CPE concentrations higher than 10 wt%, the long spacing L decreases, which is an indication of the interfibrillar segregation of CPE. This decrease can be accounted for by a decrease in the thickness of the crystalline lamellae as is discussed in the next section.

D.s.c. melting behaviour. Miscible blends of PCL with CPE or PVC exhibit two melting endotherms. For reasons explained later, the maximum of the second melting endotherm is taken as the melting temperature.

For partially miscible systems such as CPE35.6/PCL, the CPE content has little effect on the melting temperature of PCL (*Figure 19*). Since the PCL-rich phase contains little CPE35.6, the influence of this component on the melting point of PCL must be rather small or absent.

From optical microscopy, the CPE35.6/PCL 90/10 blend appears to be a one-phase system at 100°C. In spite of the low PCL content, the blend still crystallizes (spherulitically or not), an observation that is proved by differential scanning calorimetry. All the d.s.c. scans of the various compositions exhibit in the lower melting temperature range two small melting endotherms due to the low PCL fraction present in the CPE35.6-rich phase. This double melting behaviour is usually found in miscible binary blends of semicrystalline and amorphous

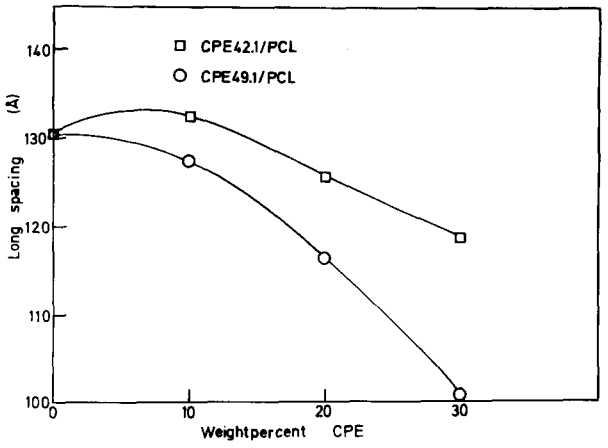

Figure 17 Variation of the long period L as measured with SAXS with composition of CPE/PCL blends after isothermal crystallization of PCL at 40°C for 14 days

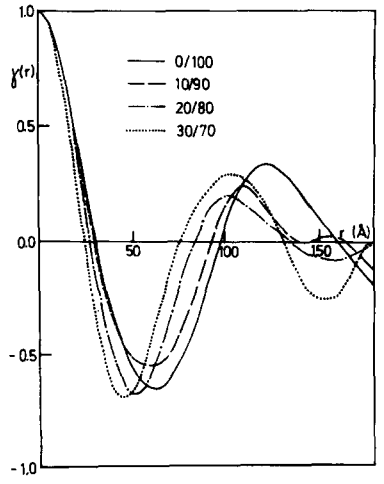

Figure 18 One-dimensional correlation function of CPE49.1/PCL blends after isothermal crystallization of PCL at 40°C for 14 days

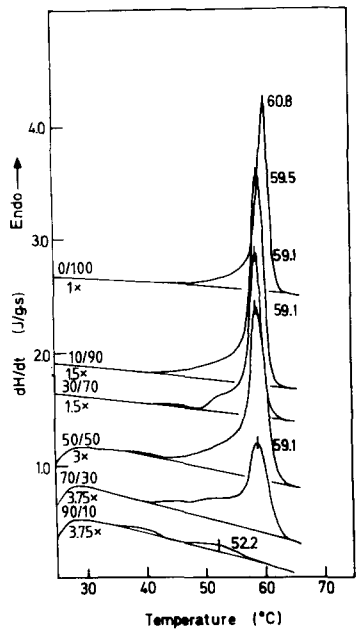

Figure 19 Influence of the CPE content on the melting behaviour of PCL in the partially miscible blend CPE35.6/PCL isothermally crystallized at 35°C for 14 days

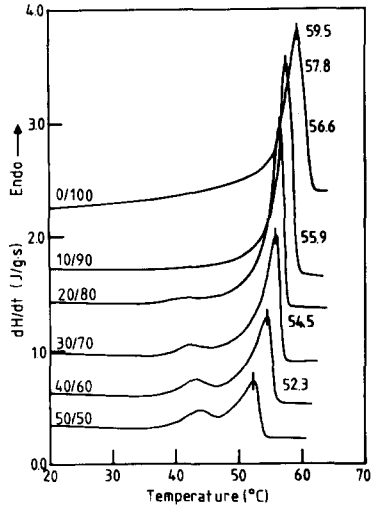

Figure 20 Influence of the CPE content on the melting behaviour of PCL in the miscible blend CPE49.1/PCL isothermally crystallized at 25°C for 14 days

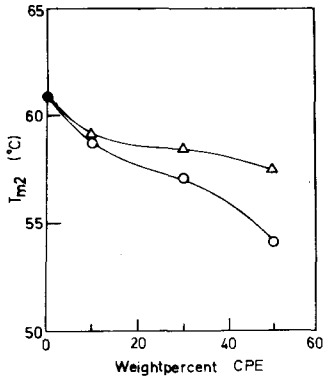

Figure 21 Influence of the CPE content on the melting behaviour of PCL in the miscible blends CPE42.1/PCL (△) and CPE49.1/PCL (○) isothermally crystallized at 35°C for 14 days

polymers. A third maximum arises when a PCL-rich phase is present in the blend.

For the miscible blends CPE42.1/PCL and CPE49.1/PCL, two melting peaks are observed in the semicrystalline mixtures (*Figure 20*) and the influence of the CPE content on the melting temperature of PCL is more pronounced than in the partially miscible blend CPE35.6/PCL (*Figure 21*). This can be explained in two ways. First of all, diluting PCL with CPE42.1 or CPE49.1 might result in thinning of the PCL lamellae. Although thermodynamic considerations predict a thickening of the crystalline lamellae in binary miscible blends due to the negative χ parameter, kinetic effects were believed to obstruct the formation of crystalline lamellae of theoretically predicted equilibrium thickness. A second reason for the decrease of the PCL melting temperature can be a melting-point depression as a consequence of a negative interaction parameter χ.

The decrease of the PCL melting temperature as a function of the blend composition is more pronounced for the CPE49.1/PCL blends, since the crystallization is more hindered as a result of the higher glass transition temperature of the blends containing CPE49.1. A second influence on the melting temperature of PCL could be an enhanced thermodynamic interaction in the CPE49.1/PCL system than in CPE42.1/PCL; a more negative value of the χ parameter results in a more pronounced melting-point depression.

These results fit very well with the SAXS data since a more pronounced decrease of the long spacing L was observed for the CPE49.1/PCL blends than for the CPE42.1/PCL blends. This was attributed to the presence of thinner lamellae in the CPE49.1/PCL blends than in the CPE42.1/PCL blends at the same composition.

Since CPE is hindering the crystallization process of PCL in the miscible blends, the melting enthalpy of PCL decreases with increasing CPE content (*Figure 22*).

The origin of the double melting behaviour of miscible polymer blends containing crystallizable and amorphous polymers has been a matter of discussion for a long time. It has been common practice to check for the occurrence of a recrystallization process using different d.s.c. scan rates in the melting range. At high d.s.c. scan rates, however, poor peak resolution is obtained and no decisive conclusions can be made. In this study, the influence of the isothermal crystallization time on the double melting behaviour was also examined. Miscible blends of CPE49.1/PCL 40/60 were molten at 180°C and isothermally crystallized at 25°C for different periods of

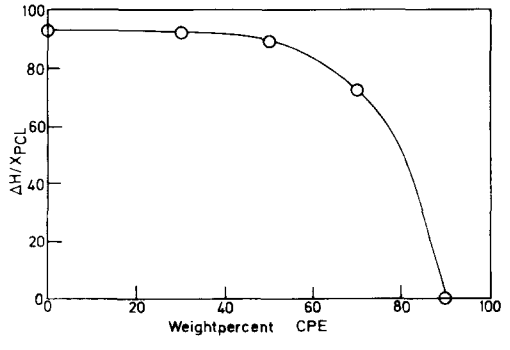

Figure 22 Influence of the CPE content on the melt enthalpy of PCL in miscible CPE49.1/PCL blends crystallized isothermally at 35°C for 14 days

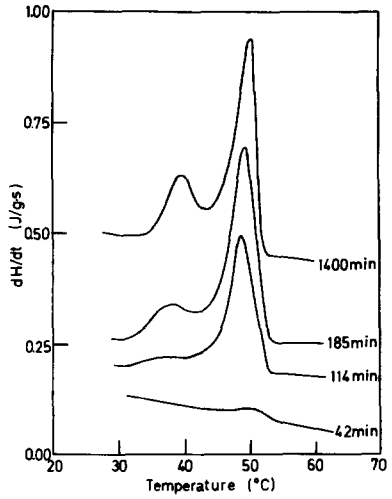

Figure 23 Double melting behaviour of CPE49.1/PCL 40/60 crystallized isothermally at 25°C for different times

time (*Figure 23*). After short crystallization times, only the second, higher melting endotherm can be observed during the melting process. The lower one only appears after prolonged crystallization times, whereas meanwhile the second higher melting endotherm has already reached a constant area and position on the temperature scale. This experiment clearly proves that the double melting behaviour cannot be attributed to partial melting followed by a recrystallization process. We therefore conclude that two types of crystalline entities (lamellae, micelles, . . .) are formed during the isothermal crystallization process. Since the melting endotherm at the lower temperature corresponds to a structure crystallizing with a lower crystallization rate, we presume that these crystals are formed after a first decrease of the PCL concentration. This decrease is due to the initial formation of the crystalline lamellae melting at higher temperatures. Consequently, the double melting behaviour is caused by the melting of two types of crystalline entities and not by the presence of a recrystallization process during the d.s.c. scan. The same experiment has been performed on other miscible binary polymer blends such as PVC/PCL, SAN/PCL and phenoxy/PCL and the same conclusions can be made for these systems.

Electron microscopic investigations. From optical microscopy and from small-angle X-ray scattering data, one can conclude that in miscible semicrystalline PCL-rich blends, CPE has to be located mainly between the crystalline PCL fibrils (stacks of lamellae).

In the miscible CPE49.1/PCL 10/90 blend, isothermally crystallized at 40°C, small fibrils can be seen (*Figure 24*). It is also clear from this electron micrograph that the spherulites are impinging and volume-filling; the ultramicrotome section was made parallel to the spherulite axis. When a section is made normal to the spherulite axis, a continuous network of segregated amorphous CPE-rich phase is observed with PCL fibrils as the dispersed phase (*Figure 25*).

It has been shown that the partially miscible system CPE35.6/PCL is essentially a two-phase system in the melt. From d.s.c. scans, it is evident that both phases can crystallize, although the CPE-rich phase contains only approximately 10 wt% PCL. This phenomenon is illustrated on an ultramicrotome section of CPE35.6/PCL 30/70 isothermally crystallized at 40°C (*Figure 26*). The PCL-rich phase forms volume-filling spherulites and the small amount of CPE is segregated interfibrillarly within this phase.

The CPE-rich phase is separated from the PCL-rich phase by a sharp phase boundary. In this CPE-rich phase, transparent domains are present (*Figure 27*) and this can be an indication for the presence of small spherulites or micelles of PCL. These small crystalline entities are

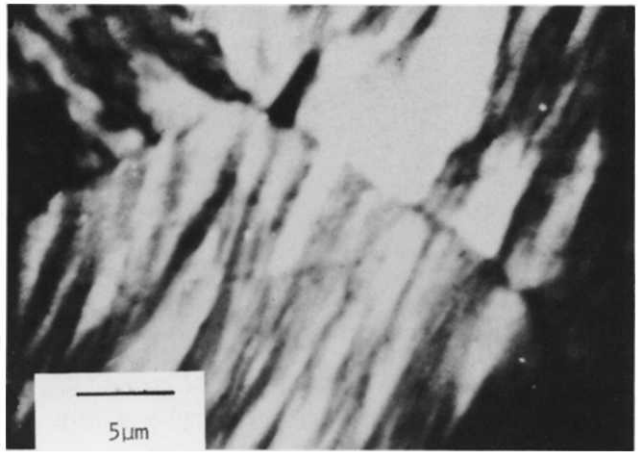

Figure 24 Transmission electron micrograph of CPE49.1/PCL 10/90 blend isothermally crystallized at 40°C for 14 days

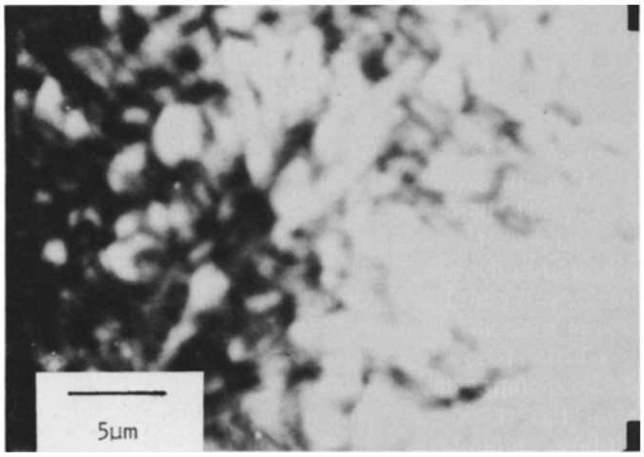

Figure 25 Transmission electron micrograph of CPE49.1/PCL 20/80 blend isothermally crystallized at 40°C for 14 days

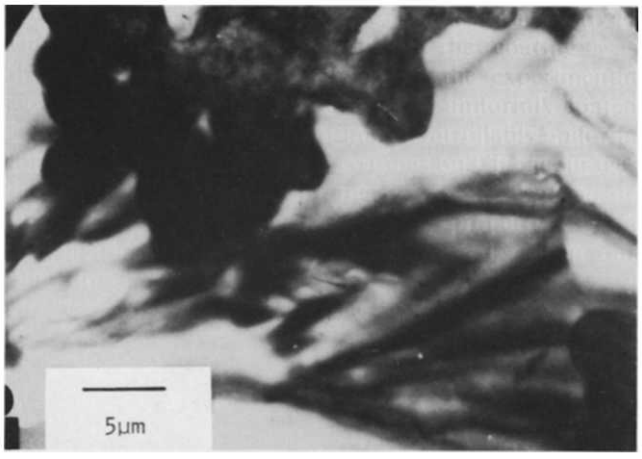

Figure 26 Transmission electron micrograph of CPE35.6/PCL 30/70 blend isothermally crystallized at 40°C for 14 days

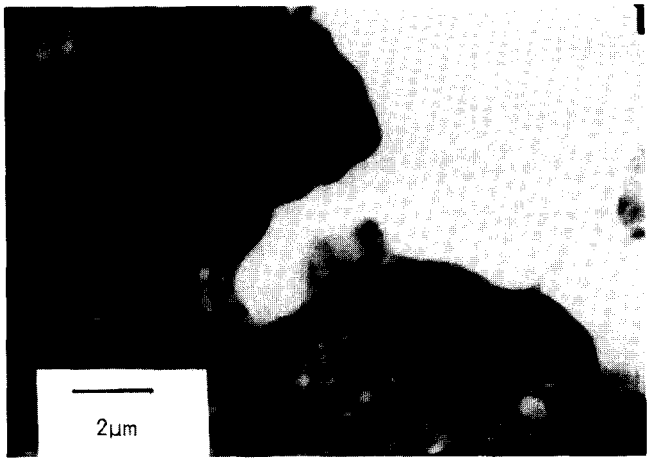

Figure 27 Transmission electron micrograph of CPE35.6/PCL 30/70 blend isothermally crystallized at 40°C at a higher magnification

responsible for the two lower melting endotherms discussed in the previous section. Moreover, these entities are not volume-filling since PCL crystallizes in the presence of a large amount of CPE (approximately 10 wt%) and from optical microscopic investigations it is known that CPE is segregated interspherulitically in this case.

CONCLUSIONS

In this study, the miscibility behaviour, crystallization kinetics and crystalline morphology of miscible and partially miscible CPE/PCL blends were examined using optical and electron microscopy, dynamic mechanical analysis, small-angle X-ray diffraction and differential scanning calorimetry.

CPE containing 49.1 wt% chlorine is miscible with PCL over the entire composition and temperature range, while CPE42.1/PCL blends exhibit a composition- and temperature-dependent phase separation behaviour. A further decrease of the chlorine content of CPE to 35.6 wt% results in a partially miscible CPE/PCL blend.

In the PCL-rich miscible blends of CPE42.1 and CPE49.1 with PCL, PCL crystallizes and forms volume-filling spherulites, while CPE is segregated in the interfibrillar domains. At higher CPE contents, CPE is segregated interspherulitically. In a partially miscible blend CPE35.6/PCL, both phases can crystallize. The PCL-rich phase forms spherulites and a small amount of CPE present in this phase is segregated interfibrillarly. The PCL fraction present in the CPE-rich phase crystallizes and forms spherulites or micelles dispersed in a CPE-rich amorphous matrix.

ACKNOWLEDGEMENTS

The authors are indebted to the Onderzoeksraad KU Leuven, NFWO for financial support given to the laboratory and the IWONL for a research grant (G.D.). They are grateful to Dr Ir. M. Vandermarliere and Ir. P. Scholiers for adapting the microdensitometer and Dr Ad Braam (DSM) for the film calibration and X-ray data processing methods.

REFERENCES

1 Khambatta, F. H., Warner, F. P., Russell, T. and Stein, R. S. *J. Polym. Sci. (A-2)* 1976, **14**, 1391
2 Stein, R. S., Khambatta, F. B., Warner, F. P., Russell, T., Escala, A. and Balizer, E. *J. Polym. Sci., Polym. Symp.* 1978, **63**, 313
3 Russell, T. P. and Stein, R. S. *J. Polym. Sci., Polym. Symp. Edn.* 1983, **21**, 999
4 Ong, C. J. and Price, F. P. *J. Polym. Sci., Polym. Symp.* 1978, **63**, 45
5 Morra, B. S. and Stein, R. S. *J. Polym. Sci., Polym. Symp. Edn.* 1982, **20**, 2261
6 Morra, B. S. and Stein, R. S. *Polym. Eng. Sci.* 1984, **24**(5), 311
7 Wenig, W., Karasz, F. E. and MacKnight, W. J. *J. Appl. Phys.* 1975, **46**(10), 4194
8 Zhikuan, C., Lianghe, S. and Sheppard, R. N. *Polymer* 1984, **25**, 369
9 Vonk, C. G. and Pijpers, A. P. *J. Appl. Crystallogr.* 1981, **14**, 8
10 Strobl, G. R. and Schneider, M. *J. Polym. Sci., Polym. Phys. Edn.* 1980, **18**, 1343
11 Olabisi, O., Robeson, L. M. and Shaw, M. T., 'Polymer–Polymer Miscibility', Academic Press, New York, 1979
12 Nojima, S., Tsutsui, H., Urushihara, M., Kosaka, W., Kato, N. and Ashida, T. *Polym. J.* 1986, **18**(6), 451
13 Keith, H. and Padden, F. J., Jr, *J. Appl. Phys.* 1964, **35**(4), 1270
14 Vandermarliere, M., Ph.D. Thesis, KU Leuven, 1986
15 Warner, F. P., MacKnight, W. J. and Stein, R. S. *J. Polym. Sci., Polym. Phys. Edn.* 1977, **15**, 2113
16 Defieuw, G., Groeninckx, G. and Reynaers, H., unpublished results